↓ **Lecture 14** [05.06.25]

4.3. Diagonalization

As a first step, we diagonalize the SSH Hamiltonian (quadratic fermions!) to obtain the spectrum and sketch the quantum phase diagram. To this end, we return to real & uniform hopping strengths t and w:

4 | $\sphericalangle$ $\hat{H}_{\text{SSH}}$ with PBC and Fourier transform

$$\tilde{x}_k = \frac{1}{\sqrt{L}} \sum_{n=1}^{L} e^{-ikn} x_n \,, \qquad x = a, b \tag{4.16}$$

$\overset{\circ}{\rightarrow}$

$$\hat{H}_{\text{SSH}} = \sum_{k \in \text{BZ}} \begin{pmatrix} \tilde{a}_k^\dagger & \tilde{b}_k^\dagger \end{pmatrix} \cdot \underbrace{\begin{pmatrix} 0 & t + we^{-ik} \\ t + we^{ik} & 0 \end{pmatrix}}_{H(k)} \cdot \begin{pmatrix} \tilde{a}_k \\ \tilde{b}_k \end{pmatrix} \tag{4.17}$$

BZ: Brillouin zone = (discrete) Circle S^1

Here $\text{BZ} = \left\{\frac{2\pi}{L}\nu \,|\, \nu = 0, \dots, L-1\right\}$.

5 | <u>Bloch Hamiltonian:</u>

$$H(k) = (t + w\,\cos k)\,\sigma^x + w\,\sin k\,\sigma^y \equiv \vec{d}(k) \cdot \vec{\sigma} \tag{4.18}$$

with Bloch vector

$$\vec{d}(k) = \begin{pmatrix} t + w\,\cos k \\ w\,\sin k \\ 0 \end{pmatrix} \tag{4.19}$$

6 | <u>Band structure:</u>

Recall our discussion of general two-band models in Section 2.1.1.

$$E_\pm(k) = \pm|\vec{d}(k)| = \pm\sqrt{t^2 + w^2 + 2tw\,\cos k} \tag{4.20}$$

There are two bands due to the two fermionic modes a_i and b_i per unit cell i.
The $\pm$ (without a constant energy offset) is a consequence of SLS (as discussed above).

7 | $\rightarrow$ <u>Phase diagram:</u>

Bandgap: $\Delta E = \min_k |E_+(k) - E_-(k)| \overset{\circ}{=} 2||t| - |w||$ (this is valid for $t, w \in \mathbb{R}$)

$\sphericalangle$ $t, w > 0 \rightarrow$ Gapless point for $w = t$, gapped insulator for $w \lessgtr t$:
(The restriction $t, w > 0$ is not important as chains with different signs are unitarily equivalent.)

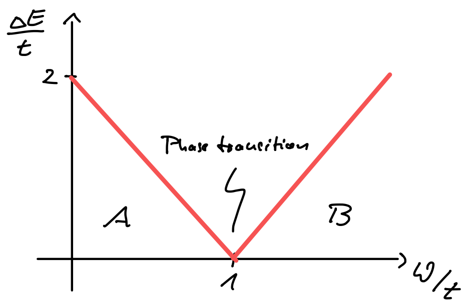

→ Unique ground state in A and B (→ no symmetry breaking)

→ How to distinguish/label the two gapped phases A and B?

We cannot use the Chern number because the Brillouin zone is S^1 in one dimensional systems (and not a torus T^2). The Chern number, however, is only defined on a two-dimensional manifold!

→ Idea:

$$\boxed{\text{Can we use SLS to define a new topological invariant?}}$$

Just like we used TRS to define the Pfaffian invariant to label the phases of the Kane-Mele model …

4.4. A new topological invariant

8 | Observation: PNS does *not constrain* $H(k)$

For any $H(k)$ the many-body Hamiltonian (4.17) conserves particle number by construction.

→ $\sphericalangle$ SLS:

$$\left[\hat{H}_{\text{SSH}}, \mathcal{S}\right] = 0 \quad \overset{4.4}{\Leftrightarrow} \quad U^\dagger H U = -H \quad \overset{4.11}{\Leftrightarrow} \quad \sigma^z H(k) \sigma^z \triangleq -H(k) \tag{4.21}$$

The last condition follows along the same lines as for time-reversal symmetry [Eq. (2.29b)] with the unitary U defined by Eq. (4.11).

9 | Eqs. (2.8) and (4.21) → Constrained Bloch vector:

$$d_z(k) \overset{\text{SLS}}{=} 0 \qquad \forall\, k \in \text{BZ} \tag{4.22}$$

→ $\vec{d}(k)$ cannot leave the x-y-plane

10 | $\sphericalangle$ Gapped phase → Normalization possible:

$$\hat{d}(k) = \frac{\vec{d}(k)}{|\vec{d}(k)|} \tag{4.23}$$

11 | → Winding number around the origin in the x-y-plane is well defined:

$$\boxed{\nu[\hat{d}] := \frac{1}{2\pi} \int_{\text{BZ}} \hat{e}_z \cdot \left[\hat{d}(k) \times \partial_k \hat{d}(k)\right] \mathrm{d}k \quad \in \mathbb{Z}} \tag{4.24}$$

¡! It is crucial that $\hat{d}$ is pinned to the x-y-plane by SLS for this to be an integer.

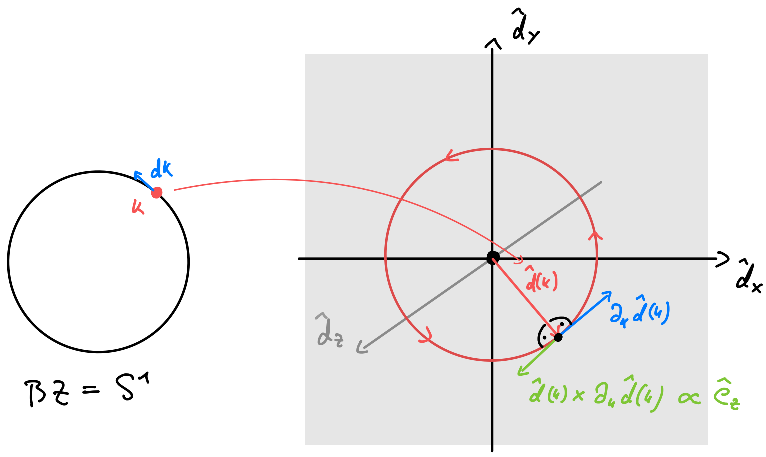

12 | The winding number ν distinguishes the Two phases:

[This follows directly from the form of the Bloch vector Eq. (4.19).]

$$\nu = \begin{cases} 0 & \text{for} \quad t > w \text{ (Phase A)} \\ 1 & \text{for} \quad t < w \text{ (Phase B)} \end{cases} \quad ☺ \tag{4.25}$$

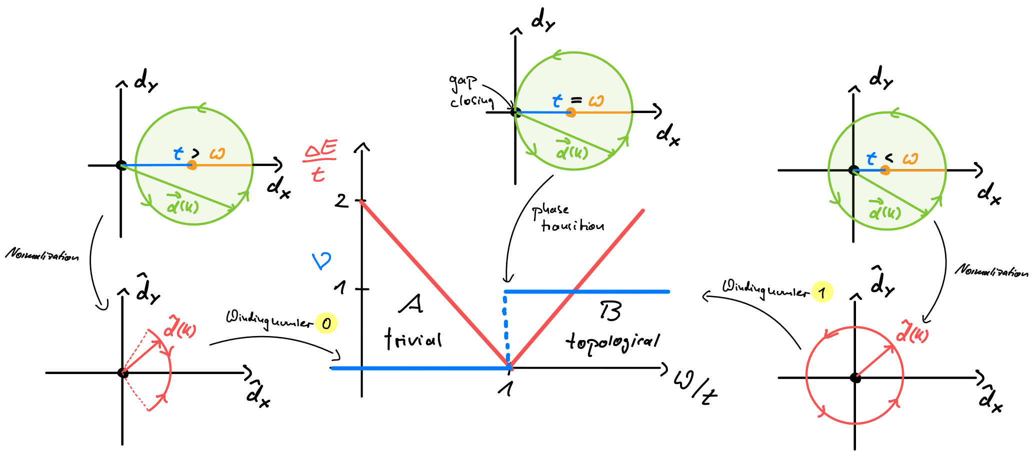

The phase A is trivial because it can be connected to the limit $t \neq 0$ and $w = 0$ without closing the gap. For these parameters, the different sites (each with two fermion modes a_i and b_i) do not couple at all and the ground state is a trivial product state.

13 | ‡ Some comments:

- Homotopy:

  We can embed this new topological invariant and the Chern number into a bigger picture if we invoke the concept of *homotopy groups* from topology. Simply speaking, the homotopy group $\pi_p(X)$ for $p = 0, 1, 2, \ldots$ and a topological space X consists of equivalence classes of continuous maps from the p-dimensional sphere S^p into X, where two maps are considered equivalent if they can be transformed into each other continuously (if the space X has a dedicated "base point" one can glue two such maps together and obtains a group structure on these equivalence classes).

  The maps we are interested in are the Bloch vectors $\hat{d}(k)$ that map the Brillouin zone onto the sphere $X = S^2$. In 1D, the BZ is S^1 so that we are interested in the homotopy group $\pi_1(S^2) = 0$ which is trivial because every circle (S^1) that you draw onto the sphere ($X = S^2$) can be continuously contracted to a point (which represents the constant map):

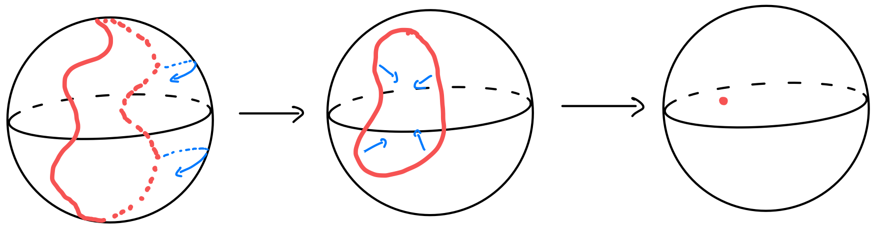

This is why there is *no* analog of the Chern number in 1D. By contrast, in 2D the BZ is a torus T^2 which we can simplify to the sphere S^2 in the continuum limit (thereby ignoring weak topological indices), so that we are interested in the homotopy group $\pi_2(S^2) = \mathbb{Z}$. Now there are different homotopy classes (corresponding to different topological phases) that are labeled by an integer – the Chern number – and distinguished by how often they wrap the target sphere when tracing over the domain sphere (which is hard to visualize, ← Section 2.1.1).

However, if we are in 1D *and* a symmetry like SLS restricts the Bloch vector to a 2D cut of S^2, namely a circle S^1, then we are interested in the homotopy group $\pi_1(S^1) = \mathbb{Z}$. The different homotopy classes consist of maps from the circle onto the circle that have different winding numbers, and therefore cannot be continuously deformed into each other:

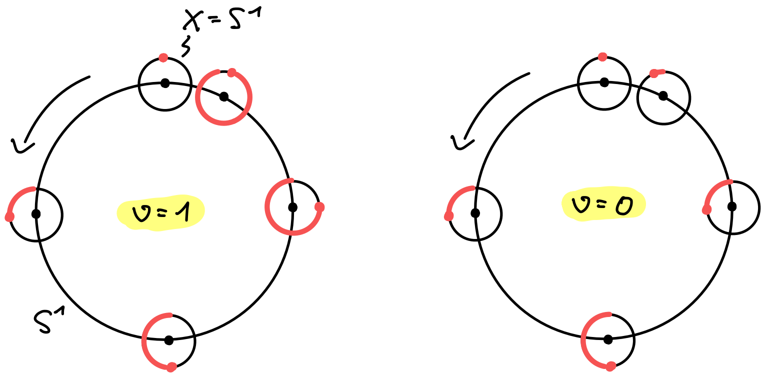

The label in this situation is the topological index ν defined above.

- Zak phase:

  We introduced the topological index ν as a winding number of the Bloch vector. When we discussed the Chern number, we arrived at it via the Berry curvature, and only later showed that in systems with two bands it can be interpreted as a winding number of the Bloch vector. This begs the question whether there is a similar expression in terms of Bloch *states* (instead of the Bloch vector) to distinguish the two phases of the SSH chain?

  The answer is "yes" and known as the *Zak phase* [127]:

$$\varphi_{\text{Zak}} = \int_{S^1} i \langle u(k)|\partial_k u(k)\rangle \mathrm{d}k \tag{4.26}$$

  where $|u(k)\rangle$ are the Bloch states of the lower (filled) band. The Zak phase is the Berry *phase* collected when traversing the 1D BZ (note that there is no Berry *curvature* in 1D).

  Remember that the Berry phase is a gauge dependent quantity and can change by multiples of 2π under continuous gauge transformations. The two phases of the SSH chain are then distinguished by the *difference* of their Zak phases:

$$\Delta\varphi_{\text{Zak}} = (\varphi_{\text{Zak}}^{\text{topological}} - \varphi_{\text{Zak}}^{\text{trivial}}) \mod 2\pi = \pi \tag{4.27}$$

  Proof: ➔ Problemset 7

  This quantity has already been measured in experiments with cold atoms in optical lattices [128].

- Polarization:

  Remember that in momentum space the *position operator* has the form $\hat{x} = i\partial_k$. The expression (4.26) for the Zak phase then looks very much like the expectation value of the position operator in the many-body ground state (= all states in the lower band filled). Indeed, the quantity $\frac{\varphi_{\text{Zak}}}{2\pi}$ is kown as ↑ *polarization* and quantifies the polarization of charge within a unit cell. The difference $\Delta\varphi_{\text{Zak}} = \pi$ between the two phases then translates to a difference in polarization by $\frac{1}{2}$ (in units of the lattice constant). And if you have a look at the distribution of hopping strengths within and between unit cells for the two cases $t > w$ and $t < w$, it is immediately clear that the electron in a unit cell will be localized either in its center (for $t > w$) or between two adjacent unit cells (for $t < w$), producing the difference of $\frac{1}{2}$ in polarization. See [2, Section 3.2.3] for more details.

4.5. Breaking the symmetry

The topological phase of the SSH chain is – supposedly – a symmetry-protected topological (SPT) phase that is protected by sublattice symmetry. According to our discussion in Section 0.5 we shoud therefore be able to transform the Hamiltonian without closing the gap into a trivial band insulator *if we break SLS*.

Let us check this explicitly ...

14 | Add a staggered chemical potential:

$$\hat{H}'_{\text{SSH}} = \hat{H}_{\text{SSH}} + \underbrace{\mu \sum_{i=1}^{L} (a_i^\dagger a_i - b_i^\dagger b_i)}_{\hat{H}_\mu} \tag{4.28}$$

Important: $[\hat{H}_\mu, \mathcal{S}] \neq 0$
To see this, remember the interpretation of SLS as bipartiteness of the coupling graph.

15 | → New Bloch vector:

$$\vec{d}(k) = \begin{pmatrix} t + w\cos k \\ w\sin k \\ \mu \end{pmatrix} \tag{4.29}$$

→ Spectrum:

$$\pm E_\pm(k) = |\vec{d}(k)| = \sqrt{\mu^2 + t^2 + w^2 + 2tw\cos k} \quad \geq \quad |\mu| \tag{4.30}$$

→ Gapped for *all* w, t (in particular $w = t$) if $\mu \neq 0$

Note that the spectrum becomes flat for $t \cdot w = 0$ and the many-body ground state of $\hat{H}_{\text{SSH}}$ for $t > 0$ and $w = 0$ is a simple product state at half-filling with one delocalized fermion per unit cell; we label this state as “trivial.” For $t = 0$ and $w > 0$ the bands are again flat and the many-body ground state can be read off the Hamiltonian: now the fermions are delocalized between two modes of *adjacent* unit cells. The family of Hamiltonians $\hat{H}'_{\text{SSH}}$ connects these two representatives adiabatically, i.e., without crossing a phase transition (→ *next point*).

16 | Connect phases without closing the gap:

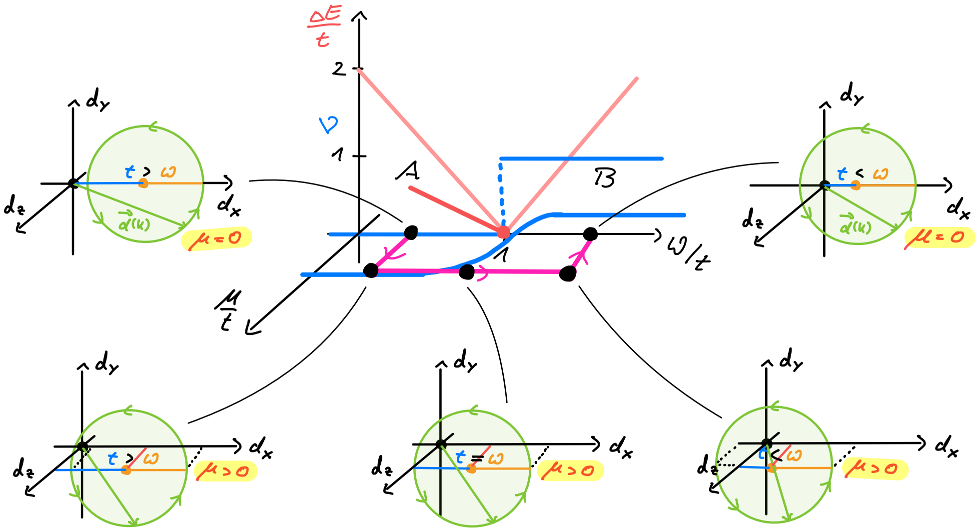

- Note that the winding number (4.24) is not quantized for $\mu \neq 0$ (= no longer an integer).
- This situation is typical for SPT phases.
- This also demonstrates that the topological phase of the SSH chain is *not* topologically ordered (= long-range entangled).

4.6. Edge modes

We now cut the SSH chain open to study one of the characteristic features of topological phases, namely the emergence of robust *edge modes* on boundaries:

Remember the inter quantum Hall states (Chapter 1), Chern insulators (Chapter 2), and topological insulators (Chapter 3) all feature robust edge modes on 1D boundaries of 2D samples. By contrast, here we consider a 1D system with 0D boundaries (points).

17 | $\triangleleft$ Open chain of length L:

For a qualitative understanding, we consider the ↑ *renormalization fixpoints* in each of the two phases (characterized by a vaninshing correlation length):

- Trivial phase (A) for $t > 0$ and $w = 0$:

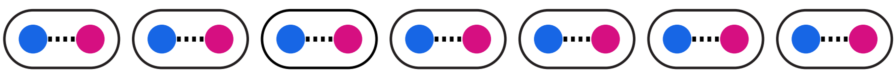

$\rightarrow$ SP Spectrum:

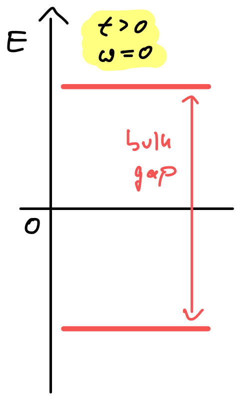

Note that due to the OBC, momentum is no longer a good quantum number, the x-axis is therefore of no relevance.

- Topological phase (B) for $t = 0$ and $w > 0$:

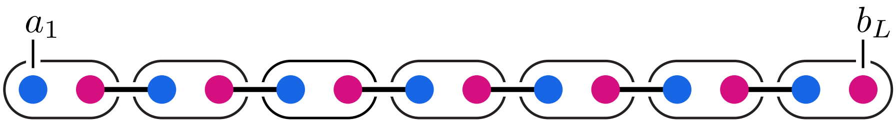

→ ⁂ *Edge modes* $\tilde{a}_l = a_1$ and $\tilde{b}_r = b_L$ commute with $\hat{H}_{\text{SSH}}$

To see this, note that a_1 and b_L no longer show up in $\hat{H}_{\text{SSH}}$.

→ 4-fold degenerate ground state space

The four ground states $|n_l, n_r\rangle$ are labeled by the occupancy $n_l = 0, 1$ and $n_r = 0, 1$ of the edge modes $\tilde{a}_l$ and $\tilde{b}_r$, i.e., $\tilde{a}_l^\dagger \tilde{a}_l |n_l, n_r\rangle = n_l |n_l, n_r\rangle$ etc.

→ SP Spectrum:

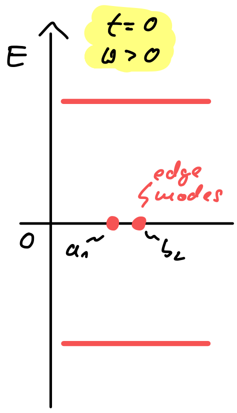

Remember that the phase is still *gapped*, despite the edge modes within the gap.

18 | Edge modes persist for $t > 0$ as long as $t < w$ (= in the topological phase):

$$\tilde{a}_l \approx \mathcal{N} \sum_{i=1}^{L} \left(-\frac{t}{w}\right)^{i-1} a_i \quad \text{and} \quad \tilde{b}_r \approx \mathcal{N} \sum_{i=1}^{L} \left(-\frac{t}{w}\right)^{i-1} b_{L-i+1} \tag{4.31}$$

The normalization $\mathcal{N}$ depends on t, w and L.

→ Exponentially localized on edges

To show that these are fermionic edge modes in the thermodynamic limit, you must first verify that they indeed describe two fermions,

$$\{\tilde{a}_l, \tilde{a}_l\} = 0\,, \quad \left\{\tilde{a}_l, \tilde{a}_l^\dagger\right\} = 1\,, \quad \left\{\tilde{a}_l^{(\dagger)}, \tilde{b}_r^{(\dagger)}\right\} = 0 \tag{4.32a}$$

$$\left\{\tilde{b}_r, \tilde{b}_r\right\} = 0\,, \quad \left\{\tilde{b}_r, \tilde{b}_r^\dagger\right\} = 1\,. \tag{4.32b}$$

Now you know that $\tilde{a}_l$ and $\tilde{b}_r$ are proper fermionic modes. They are *edge* modes because their mode weight is exponentially localized on the two edges of the chain. To show that they are edge modes *of the SSH chain*, you must show that they commute with the Hamiltonian (up to corrections that vanish exponentially in the system size):

$$\left[\tilde{a}_l, \hat{H}_{\text{SSH}}\right] = \mathcal{O}\left(\left(\tfrac{t}{w}\right)^L\right) \quad \text{and} \quad \left[\tilde{b}_r, \hat{H}_{\text{SSH}}\right] = \mathcal{O}\left(\left(\tfrac{t}{w}\right)^L\right)\,. \tag{4.33}$$

This proves the four-fold degeneracy of the ground state space for $L \to \infty$ in the topological phase $t < w$, even away from the fixpoint $t = 0$. Note that this argument fails in the trivial phase for $t > w$!

Details: ➔ Problemset 7

→ Finite-size scaling of SP spectrum:

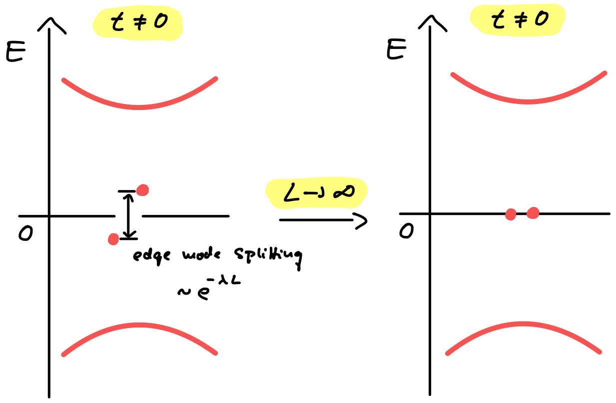

Because of the finite extend of the edge modes, there is an exponentially suppressed amplitude for a fermion located on one edge to tunnel across the chain to the other edge. The true eigenstates are therefore non-degenerate symmetric and antisymmetric superpositions of exponentially localized modes on the two boundaries. This splitting vanishes exponentially fast with the system size L. The *edge mode splitting* away from the fixpoint with $t = 0$ is therefore a *finite-size effect*.

You have observed a similar effect for the edge modes of the Kane-Mele model (Section 3.4) when studying narrow strips with open boundaries on ➔ Problemset 6: There, two of the four crossings of edge modes gapped out when the distance between the two open boundaries was small (the other two crossings were protected by time-reversal symmetry).

19 | Disorder:

The topological origin of the edge modes makes their existence & degeneracy robust against SLS-preserving disorder:

See three plots → *below*. (Use beamer to show plots.)

- ∢ No disorder:

  Plot SP spectrum of Eq. (4.10) for $w = 1 - t$ and $t \in [0, 1]$ for a chain of length $L = 40$:

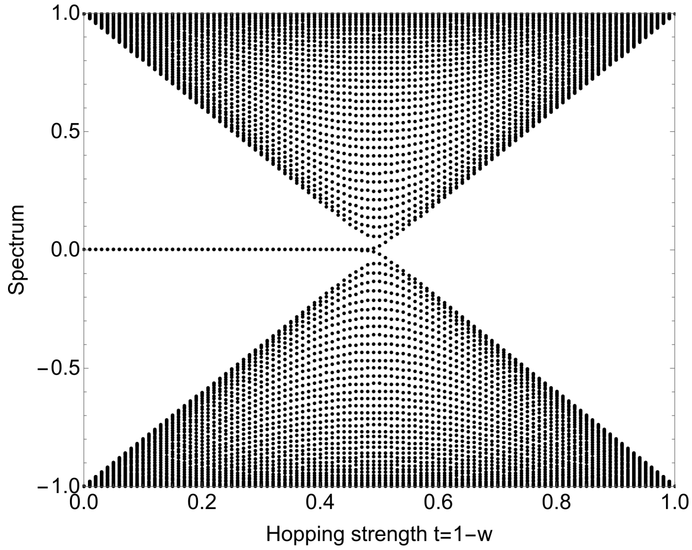

→ Degenerate zero-energy edge modes appear for $t < 0.5$ (= in the topological phase)

- $\sphericalangle$ SLS-preserving disorder:

  Plot SP spectrum with $t \mapsto t_i$ and $w \mapsto w_i$ site dependent [Eq. (4.15)]. Choose normal distributed couplings with $\langle t_i \rangle = t$, $\langle w_i \rangle = w$ and $w = 1 - t$ for $t \in [0, 1]$, with variance of 20% of the mean:

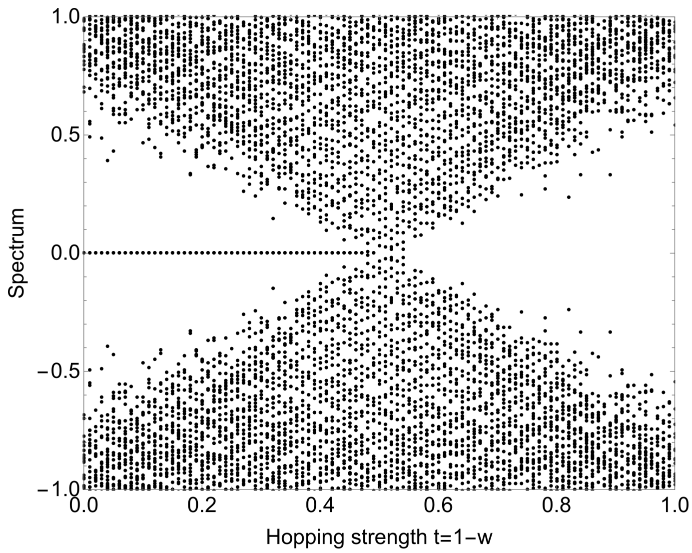

  ¡! Every spectrum (= points in a column) is computed from a *different* random configuration of couplings for a prescribed mean.

  → Bulk spectrum is scrambled but Edge modes remain degenerate and are not influenced by the disorder in the topological phase.

  Whereas the behaviour of the bulk spectrum is generic, the degeneracy of the edge modes is highly atypical and a consequence of the topological nature of the phase (and of course SLS). It is this remarkable behaviour of edge modes that is often referred to as "topologically robust ground state degeneracy" in the context of SPT phases.

- $\sphericalangle$ SLS-breaking disorder:

  Let t and w be again uniform but add a *site-dependent chemical potential* $\mu_i^a a_i^\dagger a_i + \mu_i^b b_i^\dagger b_i$ to the Hamiltonian (4.10) (this breaks SLS!). We choose μ_i^x normal distributed around zero with variance of 0.1 (remember that $w + t = 1$):

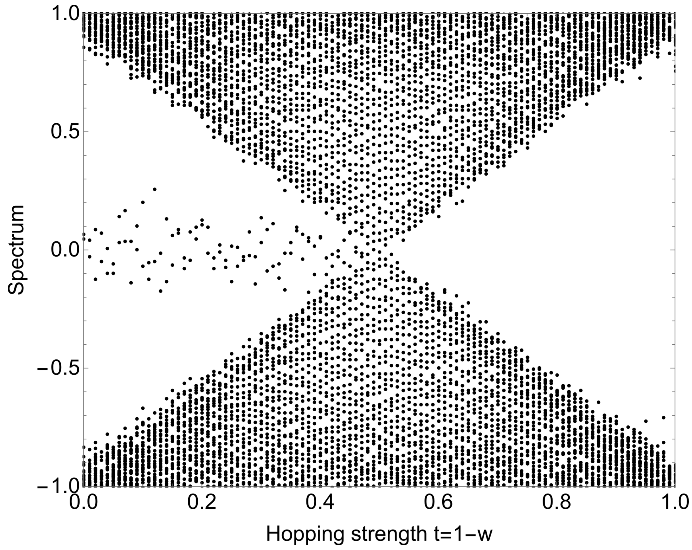

The complete spectrum (including the edge modes) is now generic as
$\rightarrow$ All degeneracies are lifted!

This demonstrates the symmetry-protection of the ground-/edge-state degeneracy.

20 | Comments:

- These results finally explain (at least partially) how the classical "experiment" in Section 0.1 (where we tried to transfer energy with a chain of coupled, classical pendulums) was motivated. Our findings above explain where the (classical) edge modes come from, and why they are robust against particular types of disorder. Recall that the energy transfer between pendulums on the boundary was perfect for disorder in the springs; this corresponds to SLS-preserving disorder in the hopping amplitudes t and w of the SSH chain. Conversely, disorder in the eigenfrequencies (= lengths) of the pendulums maps to SLS-breaking chemical potentials. (In this situation, the energy transfer was imperfect since the two edge-modes were no longer in resonance.) What remains unclear is how exactly our results for many-body *quantum systems* (described by a Hamiltonian and the Schrödinger equation) translate to *classical systems* (described by Newtonian equations of motion); we study this → *later* in **??**.
- Our study of edge modes suggests that these modes exist throughout the topological phase of the SSH chain. Note that our characterization in terms of the winding number (4.24) relies on *translation invariance* (since we make use of the Bloch Hamiltonian) – but this symmetry is explicitly broken in the scenario with SLS-preserving disorder above. The survival of the degenerate edge modes shows that the topological phase is *not* protected by translation symmetry – it is our characterization in terms of the winding number that makes use of this "auxiliary symmetry." The fact that the topological nature of the bulk influences the physics on the boundary is known as ↑ *bulk-boundary correspondence*. We encountered other examples previously; for instance, the robust boundary modes of quantum Hall states (Section 1.6) reflect the non-zero Chern number of Landau levels (which describe the bulk).
- You show on ➲ Problemset 7 analytically that edge modes of the form (4.31) persist even in the presence of SLS-preserving disorder (which explains the numerical results above).

4.7. ‡ Experiments

- The *single-particle* physics of the SSH chain has been reproduced experimentally on various platforms [128–131]. Realizing the fermionic *many-body* ground state of $\hat{H}_{\text{SSH}}$ is experimentally much more challenging (at least I am not aware of any experiments).
- The topological edge physics of the SSH chain can be applied to the problems of state transfer in quantum chains. We studied this concept theoretically in Ref. [20]; this is the paper that the classical motivation in Section 0.1 is based on. Experiments of this concept have been reported as well [132, 133].
- In 2019, we explored the single-particle physics of the SSH chain experimentally with a quantum simulator based on Rydberg atoms that interact via dipolar interactions [134]. In this experiment, we were interested in an SSH chain filled with *hardcore bosons* instead of fermions (➔ Problemset 1). While the single-particle physics (including edge states) is the same for both particle types, the many-body ground state and the symmetry classification is very different. We study the effect of interactions on topological phases in one-dimension in → Part II.